Available online at www.sciencedirect.com
ScienceDirect
International Journal of Pharmaceutics 336 (2007) 382–390
INTERNATIONAL JOURNAL OF PHARMACEUTICS
www.elsevier.com/locate/ijpharm

Pharmaceutical Nanotechnology

# Mechanistic studies on release of large and small molecules from biodegradable $SiO_2$

Reeta Viitala [a,b,*], Mika Jokinen [a,b], Jarl B. Rosenholm [a]

[a] *Department of Physical Chemistry, Åbo Akademi University, Porthansgatan 3-5, 20500 Turku, Finland*
[b] *Turku Centre for Biomaterials and Department of Prosthetic Dentistry, Institute of Dentistry, University of Turku, Itäinen Pitkäkatu 4B, 20520 Turku, Finland*

Received 7 March 2006; received in revised form 5 December 2006; accepted 6 December 2006
Available online 10 December 2006

**Abstract**

Both small and large biologically active agents were encapsulated into biodegradable sol–gel derived $SiO_2$. Both fast and slowly-eroding $SiO_2$ matrices were prepared. Propranolol represented a small molecule and a model protein, BSA (bovin serum albumin) the larger one. The release mechanisms were studied using two different dissolution media representing extreme cases with respect to the matrix erosion, free dissolution of the $SiO_2$ matrix *in sink* conditions and a dissolution medium saturated with respect to the matrix. The utilisation of the two different dissolution media as such provided information on the general release mechanisms and power law-based mathematical models supported the propranolol release results. A modified power law is suggested, where both the initially released amount and time are included. BSA was not released without matrix erosion and propranolol release was mainly diffusion-controlled, although the matrix dissolution was needed for $R = 3$ monoliths due to closed pores. It is also shown that for $R = 30$ microparticles propranolol release was partly matrix erosion controlled.


*Keywords:* Silica; Sol–gel; Drug delivery; Release mechanism; *In vitro* dissolution

## 1. Introduction

Amorphous, sol–gel derived $SiO_2$ matrices are known to be compatible with and degradable in living tissue, as well as in corresponding simulated physiological conditions (Kortesuo et al., 2000a; Meseguer-Olmo et al., 2002). The low temperature liquid phase processing provides possibilities to encapsulate different types of biologically active agents into $SiO_2$. Small drug molecules (Böttcher et al., 1998; Ahola et al., 2000; Radin et al., 2001), proteins (Arnir et al., 1994; Nicoll et al., 1997; Santos et al., 1999; Bhatia et al., 2000; Keeling-Tucker et al., 2000; Kadnikova and Kostic, 2001; Flora and Brennan, 2001), cells (Pope et al., 1997; Al-Saraj et al., 1999; Sglavo et al., 1999; Conroy et al., 2000), viruses (Koskinen et al., 2003) and other biologically active agents, some of them being highly sensitive to the surrounding conditions, have been successfully encapsulated into the sol–gel derived $SiO_2$. Furthermore, the possibility to adjust the degradation rate on large scale in simulated physiological conditions (Ahola et al., 2001; Viitala et al., 2005a) and to prepare amorphous $SiO_2$ in several morphologies (Kortesuo et al., 2000a,b) (e.g., as injectable microparticles or implantable rods) makes the $SiO_2$ sol–gel technique an attractive alternative for the delivery of biologically active agents.

It is shown that viruses retain their biological activity and viability in wet $SiO_2$ gel for several weeks (Koskinen et al., 2002). This suggests general potential of the conventional sol–gel method in encapsulation of corresponding large biologically active agents, e.g., cells, bacteria or large proteins. The release of biologically active agents from nanoporous $SiO_2$ matrix is mainly governed by a combination of $SiO_2$ matrix degradation and diffusion whose influence on the final release behaviour varies case by case. If the size of the encapsulated molecules is bigger than the pore size of the matrix (e.g., viruses and proteins encapsulated in $SiO_2$ matrix) or if the drug molecules are encapsulated into closed pores matrix degradation is needed before drug is released. In the case of diffusion both drug molecules

* Corresponding author at: Turku Centre for Biomaterials and Department of Prosthetic Dentistry, Institute of Dentistry, University of Turku, Itäinen Pitkäkatu 4B, 20520 Turku, Finland. Tel.: +358 2 333 8530; fax: +358 2 333 8750.
*E-mail address:* reevii@utu.fi (R. Viitala).

0378-5173/$ – see front matter © 2006 Elsevier B.V. All rights reserved.
doi:10.1016/j.ijpharm.2006.12.008

and matrix degradation products diffuse out from the matrix. Diffusion occurs through water filled pores and in bulk eroding matrixes the diffusion environment is changing all the time because of matrix degradation (Göpfrich, 1997; Göpferich and Langer, 1995; Lee et al., 2003). Parameters like porosity, chemical structure and encapsulated drug molecule affect the matrix degradation and their influence have to be considered case by case for versatile systems, such as sol–gel derived $SiO_2$. We have recently shown that it is relatively easy to adjust the dissolution of $SiO_2$ on a large scale in simulated physiological conditions using the conventional sol–gel parameters; water-to-alkoxide ratio, solvent amount, catalyst concentrations and the process parameters, such as aging and drying (Viitala et al., 2005a,b). It is also known that *in vivo* $SiO_2$ dissolves into bodily fluids as silicic acid without extra cleavage steps and it is mainly removed through urine in soluble form, which makes $SiO_2$ matrixes an attractive option for drug delivery applications (Lai et al., 1998).

In surface erosion, material is lost from the matrix exterior surface and in an ideal case the erosion rate is directly proportional to the external surface area. For thin, flat slabs that retain the constant external surface, the matrix erosion is constant showing zero-order kinetics and homogenously encapsulated molecules must also follow zero-order release. For spheres and cylindrical rods the release will decline towards the end (Siepmann and Göpferich, 2001; Tamada and Langer, 1993). In bulk erosion, the material is lost from entire matrix volume and water penetrates into matrix faster than the matrix is degraded. The bulk erosion rate depends on the total amount of material and generally decreases as material is depleted. Porous and hydroscopic matrices, such as sol–gel derived $SiO_2$ matrices, degrade mostly by a combination of both suggested ideal cases, as do most of the degradable drug delivery devices (Kortesuo et al., 2001a; Siepmann and Göpferich, 2001). Zero-order release kinetics of biologically active agents may also be obtained by bulk erosion with a suitable combination of other matrix properties, such as water and drug diffusion, polymer swelling and degradation (Siepmann and Göpferich, 2001).

The aim of this work is to study the release mechanisms of different types of biologically active agents from sol–gel derived $SiO_2$ with specific emphasis on the influence of $SiO_2$ matrix erosion on the release. Propranolol represents a small drug molecule and BSA (a model protein) a larger molecule that are encapsulated into sol–gel derived $SiO_2$ matrices. Both spray-dried microparticles and monoliths cast in the moulds were prepared. The experimental method is based on the utilisation of two dissolution media simulating the extreme cases of matrix dissolution. The drug release and matrix erosion are studied *in vitro* in Tris buffer (pH 7.4 at 37 °C) *in sink* conditions ($SiO_2 < 30$ ppm) allowing free dissolution of the matrix and in $SiO_2$-saturated buffer (130 ppm $SiO_2$), where the matrix dissolution is prevented. The traditional power law and a new modified power law where the initial release (burst or lag time) effects are taken into account are used in comparative analysis of the release mechanism. Experimental results combined with results obtained from mathematical models are used to evaluate the release mechanisms.

## 2. Materials and methods

### 2.1. Material preparation

The sol–gel technique is used to produce $SiO_2$ monoliths and microparticles. Matrices were prepared by the hydrolysis and condensation of tetraethoxysilane (TEOS 98%, Aldrich). BSA and propranolol were added into the sols. Bovine serum albumin BSA (bovine albumin extracted from buffalo blood) is used as a model protein. It has a molecular weight of 68 kDa. Brown and Shockley (1982) have constructed a model of BSA as having a cigar shape in size 4 nm × 14 nm (Friedli, 1996). The isoelectric point of BSA is at pH 4.7. Propranolol (1-(isopropylamino)-3-(1-naphthyloxy)-2-propanol hydrochloride) was used as a small drug molecule, it has the molecular weight of 295 g/mol. Propranolol has the $pK_a$ value of 9.4. The amount of BSA or propranolol was 5, 7 or 10 wt.% of the theoretical $SiO_2$ amount in the sol (1 mol TEOS = 1 mol $SiO_2$). The sol compositions are presented in Tables 1 and 2.

Hydrochloric acid (HCl) and sodium hydroxide (NaOH) were used to adjust the sol pH. The hydrolysis time in Tables 1 and 2 means the time needed to achieve a homogeneous sol at room temperature under magnetic stirring. The process starts at acidic $pH_1$. A two-step catalysis process was used in the encapsulation of BSA. The initial sol $pH_1$ was low and before adding the BSA the $pH_1$ was raised to $pH_2$ in order to avoid the protein denaturation. After the pH adjustment, BSA was added into the sol as an aqueous solution, which raised simultaneously the water-to-TEOS value of the sol from $R_1$ to $R_2$. Only one pH was used in the propranolol containing sols. The sols used in the microparticle preparation (Tables 1 and 2, group B) were aged at 40 °C for 65–67 h before adding the drug molecules into the sol.

Monoliths were prepared by drying the sol in a mould. The sol was injected into moulds where aging and drying occurred. The sols and formed gels were aged and dried at 4 °C or at 40 °C and 40% relative humidity. No further heat-treatment was used. The aging and drying process of the monoliths is a slow and unforced process done at constant conditions, where the gel structure is formed. Monolithic gels (as rods and tablets) were dried to the constant weight. The BSA containing monoliths and Am06–08 specimens were rods and Bm12–15 tablets. The amount of cast sol per mould was 170 μl. Microparticles were prepared by spray-drying the sols with a mini spray dryer (B-191, Büchi Labortechnik AG, Switzerland). The following process parameters were used: pump 16%, aspirator 95%, and flow 600 l/h. The nozzle temperature was 120 °C and the outlet temperature was under 75 °C.

### 2.2. In vitro matrix dissolution and drug release studies

Matrix degradation was measured as $SiO_2$ dissolution. $SiO_2$ dissolution and drug release was studied *in vitro* by immersing silica monoliths ($R = 30$: 16–18 mg and $R = 3$: 48–53 mg) and microparticles (10–20 mg) in 0.005 M Tris (Trizma® preset Crystals, Sigma) buffer at pH 7.4 *in sink* conditions and in the same buffer saturated with $SiO_2$ ($SiO_2$ 120–130 ppm). *In sink* conditions for dissolved Si-species is below 20% of the

Table 1
Sol compositions of BSA containing monoliths and microparticles

| Sample name | $R_1$ | Sol $pH_1$ | EtOH/$TEOS_1$ (mol) | Hydrolysis time[a] (min) | Sol aging time (h) | $R_2$ | EtOH/$TEOS_2$ (mol) | Sol $pH_2$ | BSA (wt.%) | Aging and drying, $T$ (°C) | Spray drying, $T$ (°C) |
|---|---|---|---|---|---|---|---|---|---|---|---|
| A-group ($R_1$ = 19–22; $pH_1$ 2.8) | | | | | | | | | | | |
| Monoliths | | | | | | | | | | | |
| Am01 | 22 | 2.8 | – | 140 | – | 30 | – | 5.2 | 7 | 4 | – |
| Am02 | 19 | 2.8 | – | 140 | – | 30 | – | 5.3 | 10 | 4 | – |
| Microspheres | | | | | | | | | | | |
| As03 | 22 | 2.8 | – | 140 | – | 30 | – | 5.3 | 5 | – | 120 |
| As04 | 22 | 2.8 | – | 140 | – | 30 | – | 5.4 | 7 | – | 120 |
| B-group ($R_1$ = 2; $pH_1$ 2) | | | | | | | | | | | |
| Microspheres | | | | | | | | | | | |
| Bs05 | 2 | 2 | 1 | 15 | 65 | 20 | 1.8 | 6.3 | 5 | – | 120 |

[a] Time needed to achieve homogeneous sol, $R$: $H_2O$/TEOS mol ratio of the sol; $R_1$: the initial $R$ of the sol; $R_2$: $R$ of the sol after dilution and/or BSA adding; $pH_1$: calculated initial pH of the sol; $pH_2$: the measured pH of the sol after the pH adjustment for BSA; EtOH/TEOS: ethanol/TEOS mol ratio of the sol.

$SiO_2$ solubility corresponding to $c(SiO_2)$ <30 ppm. They represent two extreme cases, a free dissolution of the $SiO_2$ matrix and no or minimal dissolution of $SiO_2$, respectively. The total amount of $SiO_2$ in the monoliths was calculated from the known sol volume and TEOS amount per monolith. For the monoliths, typically 85% of the sample weight is $SiO_2$. Based on our earlier dissolution studies the amount of $SiO_2$ in the microparticles is about 60% of the sample weight. This is due to residuals, like water and ethanol and unreacted or partly reacted alkoxide species that are always left in non heat-treated $SiO_2$ xerogel matrices.

The $SiO_2$ saturated Tris buffer was prepared by first dissolving the sol–gel derived $SiO_2$ microparticles into Tris buffer until a concentration of 120–130 ppm $SiO_2$ was achieved. The buffer was subsequently filtered to remove remaining microspheres. The influence of high $SiO_2$ concentration in the buffer properties was characterised. Solubility of the studied biologically active agents, viscosity and surface tension of the buffer was measured and compared with the corresponding values for the buffer without $SiO_2$. There were no differences between these two buffers. The total amount of drugs encapsulated into $SiO_2$ was very low compared with the solubility of the drugs in the both buffers. The Tris buffer was sterilized at 121 °C before use. In the case of $SiO_2$-saturated Tris buffer, the $SiO_2$ was added after the sterilisation. The dissolution studies were done in the water bath at 37 °C, where dissolution bottles were shaken at constant speed. The Si concentration was measured with a spectrophotometer (UV-1601, Shimadzu) analysing the molybdenum blue complex absorbance at 820 nm. The BSA concentration was determined directly by measuring the absorbance at 220 nm and propranolol at 227 nm with a spectrophotometer (UV-1601, Shimadzu).

### 2.3. Release models

The modelling of release is an extensively studied topic in the drug delivery. Different empirical and semi-empirical models have been developed, such as the classical Higuchi equation (Higuchi, 1961) and the so-called power law (Siepmann and Peppas, 2001) based on Fick's second law of diffusion and assumptions that diffusion coefficient is concentration-independent and drug distribution is homogeneous in the device. Although the power law has its limitations, it is considered to be more useful in the comparative studies providing explanations also for matrices that do not fulfil the presumptions of the Higuchi model (Harland et al., 1988; Siepmann and Peppas, 2001). The general form of the power law is:

$$\frac{M_t}{M_\infty} = kt^n \quad (1)$$

which includes $M_t$ the cumulative drug released at time $t$, $M_\infty$ the cumulative drug release at infinite time, $k$ being a constant depending on the structural and geometrical characteristics and the release exponent $n$ indicating the mechanism of drug release. This equation can be used until 60% of the drug has been release (Peppas, 1985). The exponent value depends slightly on the geometry of the device and it is shown that exponent values between 0.43 and 0.5 are indicative of diffusion-controlled

Table 2
Sol compositions of propranolol containing monoliths and microparticles

| Sample name | $R_1$ | Sol $pH_1$ | EtOH/$TEOS_1$ (mol) | Hydrolysis time[a] (min) | Sol aging time (h) | $R_2$ | EtOH/$TEOS_2$ (mol) | Propranolol (wt.%) | Aging and drying, $T$ (°C) | Spray drying, $T$ (°C) |
|---|---|---|---|---|---|---|---|---|---|---|
| A-group ($R_1$ = 30; $pH_1$ 2.8) | | | | | | | | | | |
| Monoliths | | | | | | | | | | |
| Am06 | 30 | 2.8 | – | 110 | – | 30 | – | 5 | 4 | – |
| Am07 | 30 | 2.8 | – | 110 | – | 30 | – | 7 | 4 | – |
| Am08 | 30 | 2.8 | – | 110 | – | 30 | – | 10 | 4 | – |
| Microspheres | | | | | | | | | | |
| As09 | 30 | 2.8 | – | 110 | – | 30 | – | 5 | – | 120 |
| As10 | 30 | 2.8 | – | 110 | – | 30 | – | 7 | – | 120 |
| As11 | 30 | 2.8 | – | 110 | – | 30 | – | 10 | – | 120 |
| B-group ($R_1$ = 2–3; $pH_1$ 2) | | | | | | | | | | |
| Monoliths | | | | | | | | | | |
| Bm12 | 3 | 2 | – | 60 | – | 3 | – | – | 40 | – |
| Bm13 | 3 | 2 | – | 60 | – | 3 | – | 5 | 40 | – |
| Bm14 | 3 | 2 | – | 60 | – | 3 | – | 7 | 40 | – |
| Bm15 | 3 | 2 | – | 60 | – | 3 | – | 10 | 40 | – |
| Microspheres | | | | | | | | | | |
| Bs16 | 2 | 2 | 1 | 15 | 65 | 14 | 1.8 | 5 | – | 120 |
| Bs17 | 2 | 2 | 1 | 15 | 66 | 14 | 1.8 | 7 | – | 120 |
| Bs18 | 2 | 2 | 1 | 15 | 67 | 14 | 1.8 | 10 | – | 120 |

[a] Time needed to achieve homogeneous sol; $R$: $H_2O$/TEOS mol ratio of the sol; $R_1$: the initial $R$ of the sol; $R_2$: $R$ of the sol after sol dilution; $pH_1$: calculated initial pH of the sol; EtOH/TEOS: ethanol/TEOS mol ratio of the sol.

release. Higher $n$ values (0.85–1.0) are typical for drug transport in swelling polymer devices. $n = 1.0$ indicates actually zero order drug release kinetics, which can be achieved also with matrix erosion controlled systems (Siepmann and Peppas, 2001). The $n$ values between 0.5 and 1.0 are indicative of anomalous transport behaviour including both diffusion and swelling or erosion (Siepmann and Peppas, 2001). Peppas has suggested that the $n$ values below 0.50 are indicative of porous matrix structure (Peppas, 1985). Transport of drug molecules in typical nanoscale pores of sol–gel derived $SiO_2$ may also show square root of time dependence as shown, e.g., by Kortesuo et al. (2001b). However, although the typical $SiO_2$ may show square root of time kinetics of drug release, it is known that the porous and amorphous materials, such as $SiO_2$ that has heterogeneous pores with respect to form, length, diameter, fractality and surface roughness, may cause unexpected transport behaviour differing from diffusion as compared to, structures that have well-defined and smoother pores (Andrade et al., 1997; Kumar and Yashonath, 2000).

The burst effect which is the initial, short-time release of large amount of drug before a more stable and slower release phase, has not been taken into account in all release models. Huang et al. have introduced a modified power law model that includes an additional burst parameter, $\alpha$: $M_t/M_\infty = kt^n + \alpha$. The release profile is shifted vertically by $\alpha$ accounting for a rapid jump in concentration at $t = 0$ (Huang and Brazel, 2001). The initial release phase may also be slower than the longer lasting main release phase, i.e., lag time is sometimes observed. Both burst and lag time differ from the main release phase and lag time may also last a relatively long time. In order to take this initial release, either burst or lag time, into account we suggest a modified power law model:

$$\frac{M_t - M_2}{M_\infty} = k(t - t_2)^{n_B} \quad (2)$$

where $M_t$ is the cumulative release at time $t$, $M_2$ the amount released within the initial release phase (that differs from the main release phase), $M_\infty$ the cumulative drug release at infinite time, $k$ the constant depending on the structural and geometrical characteristics of the device, $t_2$ the end point time of the initial release and $n_B$ is the release exponent characteristics for the mechanism of drug release after the initial release. By plotting the $\ln(M_t - M_2/M_\infty)$ versus $\ln(t - t_2)$ the $n_B$ can be calculated from the slope of this curve. The values of $n_B$ are interpreted in the same way as the values of $n$ (in power law), which are characteristic for the drug release mechanism, but $n_B$ describes the release, which occurs after the initial release.

## 3. Results

### 3.1. $SiO_2$ degradation by dissolution

As expected, $SiO_2$ matrix dissolution was not observed in the $SiO_2$-saturated Tris buffer. The dissolution of the matrix in Tris buffer *in sink* conditions is presented as cumulative dissolution of $SiO_2$ in Figs. 1 and 2. The matrix dissolution results showed great variation based on the water-to-TEOS ratio and/or processing method resulting either in monolithic rods and tablets or microparticles. There was no significant difference in the $SiO_2$ dissolution between the BSA- and propranolol-containing monoliths made at high water-to-TEOS ratios, $R_2 = 30$ (Am01, Am02, Am06, Am07 and Am08, Fig. 1). The concentration of the encapsulated biologically active agents did not have a significant influence on the $SiO_2$ monolith dissolution, although higher concentration of propranolol made the matrix dissolve a bit faster.

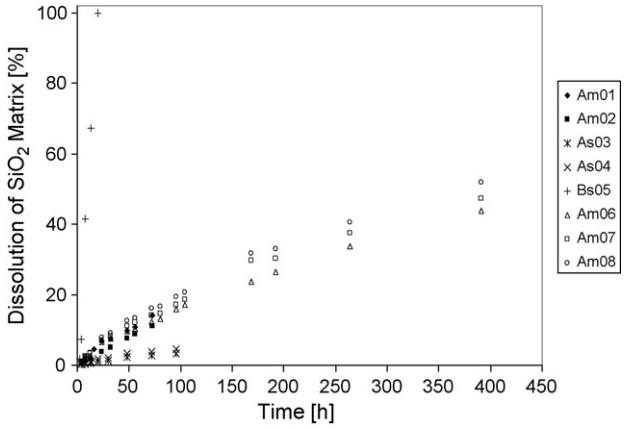


Fig. 1. $SiO_2$ dissolution of Am01–08 matrices in Tris buffer *in sink* conditions.

BSA containing $SiO_2$ microparticles prepared at high water-to-TEOS ratios, $R_1 = 22$ (As03 and As04) dissolved more slowly than microparticles prepared at low water-to-TEOS ratios, $R_1 = 2$ (Bs05) as seen in Fig. 1. Low water-to-TEOS ratio propranolol-containing microparticles also dissolved very fast (Bs16–18, Fig. 2). In the case of matrixes prepared at $R = 30$ the effect of propranolol amount to the matrix degradation rate was much greater in microparticles (As09–11) than in monoliths (Am06–08). The higher the propranolol concentration the faster the $SiO_2$ dissolution. This can be explained by the typical dense structure of the $SiO_2$ microparticles (Viitala et al., 2005a) where any extra additive makes the structure more heterogeneous. Some kind of two-phase behaviour is visible in the release profile (As09–11), i.e., faster dissolution in the beginning (about up to 250 h) followed by a more linear

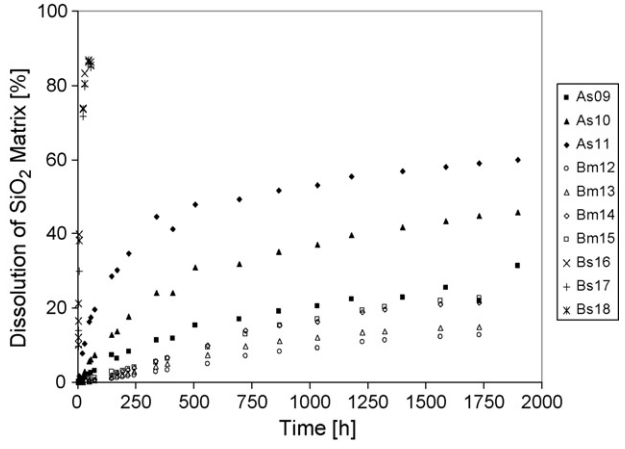


Fig. 2. $SiO_2$ dissolution of As09–Bs18 matrices in Tris buffer *in sink* conditions.

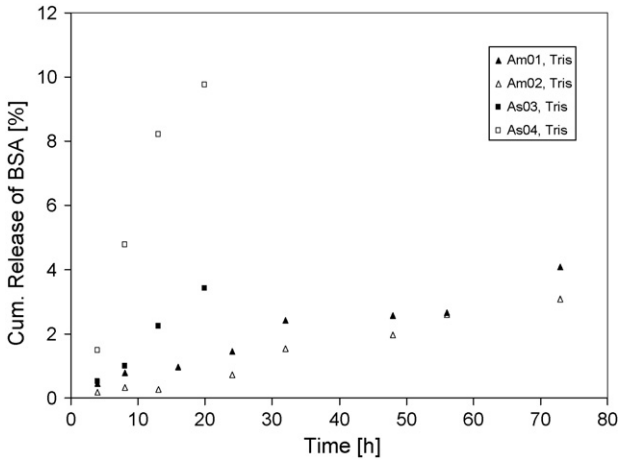


Fig. 3. BSA release *in sink* conditions from monoliths Am01–02 and microparticles As03–04.

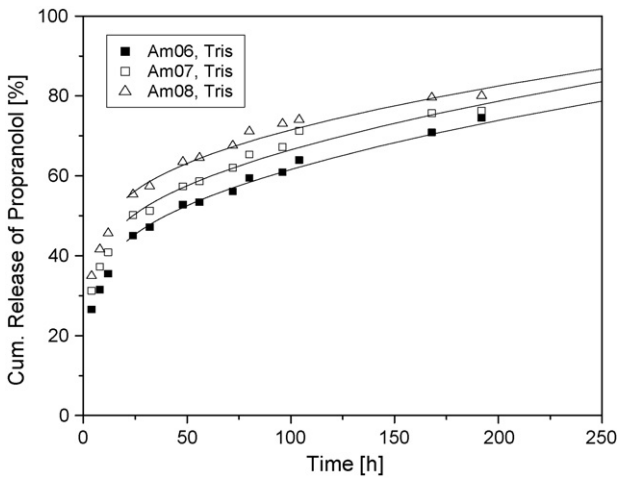


Fig. 4. Propranolol release *in sink* conditions from monoliths Am06–08. Lines are the corresponding calculated modified power law release profiles after the initial release phase.

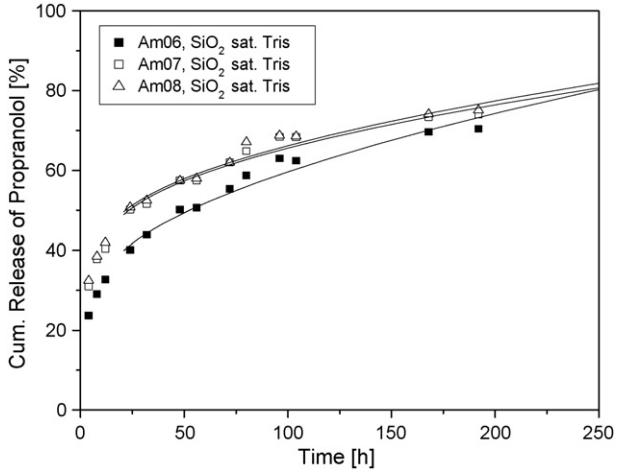


Fig. 5. Propranolol release in $SiO_2$ saturated Tris buffer from monoliths Am06–08. Lines are the corresponding calculated modified power law release profiles after the initial release phase.

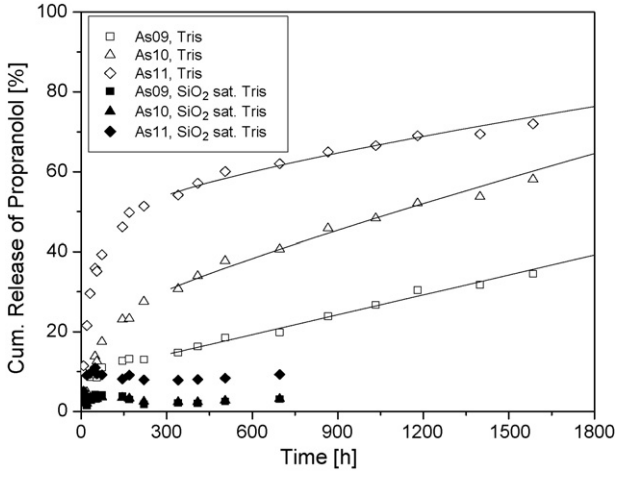


Fig. 6. Propranolol release in Tris (*in sink* conditions) and in $SiO_2$ saturated Tris from the microparticles As09–11. Lines are the corresponding calculated modified power law release profiles after the initial release *in sink* conditions.

phase. The matrix dissolution rates of monoliths made at low water-to-TEOS ratios, $R_1 = 3$ (Bm12–15) show also some propranolol concentration dependence, matrix degradation rate increased as the propranolol amount increased (Fig. 2).

### 3.2. BSA release

BSA release from monoliths and microparticles ($R = 19$–$22$) is presented in Fig. 3. The release of BSA occurs only *in sink* conditions and no release is observed in $SiO_2$-saturated buffer. Pores in the $SiO_2$ matrix are not large enough for significant diffusion of BSA without the $SiO_2$ matrix dissolution. This indicates that release occurs due to the $SiO_2$ matrix dissolution, by erosion-control. Fig. 3 shows also a good example on the lag time that is observed for Am02. The observed faster release from microspheres than from the monoliths is most likely due to the denser structure of microspheres (Viitala et al., 2005a), where the presence of BSA produces more heterogeneity in $SiO_2$ structure than in the case of the monoliths.

In the case of fast dissolving microparticles (Bs05, $R = 2$) with low water-to-TEOS ratio the BSA release is fast both *in sink* conditions and in $SiO_2$-saturated buffer, BSA is totally released in both buffers after 2 h dissolution (not shown). BSA release is even faster than the matrix degradation presented in Fig. 1. Because the BSA release seems to be even faster than the $SiO_2$ matrix dissolution, it is likely that the real encapsulation has not occurred in the $SiO_2$ microparticles with low water-to-TEOS ratio.

### 3.3. Propranolol release

The measured cumulative release of propranolol *in sink* conditions and in $SiO_2$-saturated buffer are shown as dots and the modelled release as line graphs in Figs. 4–7. Modelled release graphs are calculated based on the new modified power law and calculated variables are presented in Table 3. The difference in the propranolol release *in sink* conditions and $SiO_2$-saturated buffer is insignificant for the monoliths made at high water-to-TEOS ratios, $R = 30$ (Am06–08, Figs. 4 and 5), i.e., the

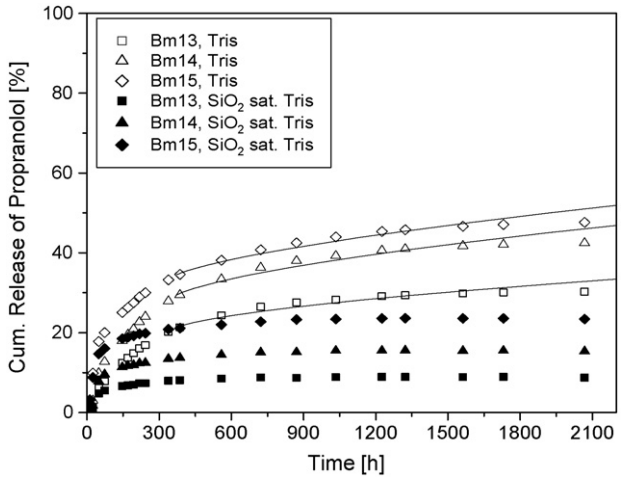


Fig. 7. Propranolol release in Tris (*in sink* conditions) and in $SiO_2$ saturated Tris from monoliths Bm13–15. Lines are the corresponding calculated modified power law release profiles after the initial release *in sink* conditions.

dissolution of the $SiO_2$ matrix had no effect and the release differs clearly from that of larger BSA molecules. This result together with two other observations suggests that the propranolol release from Am06–08 is governed by out-diffusion from the pores: (1) $SiO_2$ matrix dissolution (Fig. 1) is slower than the propranolol release and (2) $n_B$ values (Table 3; $n_B = 0.5 \pm 0.07$ for all propranolol concentrations) are typical for the diffusion-controlled release. The $n_B$ is obtained by subtracting 12 first hours of the release. If the burst or the initial release phase is not removed from the release curve, a low $n$ value of 0.2 with no clear physical meaning is obtained. The burst cannot be perfectly defined, but the release rate is approximately four times faster than within next 12 h and the fitting to linear curve in ln–ln graph does not provide acceptable correlation factor for 0–24 h initial release. The used experimental dissolution media support our choice, 0–12 h, by indicating same burst both in the $SiO_2$-saturated buffer and in the buffer *in sink* conditions. In addition, the $SiO_2$ matrix dissolves only 2–3% *in sink* conditions within 12 h. The dissolution (about 40% at 250 h) does not seem to affect the mechanism and this is suggested to depend on the bulk erosion mechanism that includes a strong diffusion component also in the matrix erosion.

In the case of the microparticles with high water-to-TEOS ratio (As09–11, $R_1 = 30$, Fig. 6) the propranolol release in the $SiO_2$-saturated buffer is low, only 3 wt.% for (As09 and As10) and 8 wt.% for (As11) and the released amount does not increase after the initial burst. However, propranolol is increasingly released *in sink* conditions. These results indicate that the $SiO_2$ matrix dissolution is needed for the release. The propranolol release during the initial release phase is lowest for the $SiO_2$ microparticles containing 5% propranolol and highest for microparticles with 10% propranolol. The initial release phase was chosen to be between 0 and 220 h. The release of propranolol was faster than $SiO_2$ matrix dissolution until 220 h. The $n_B$ value for microparticles containing 5% propranolol indicates matrix-erosion controlled release $n_B = 1.00$, and for 7% and 10% propranolol $n_B = 0.86$ and 0.74, respectively. Also the $n_B$ values are logical with the propranolol amount; increasing amount of propranolol seems to increase the effect of diffusion component. If the initial release phase is not subtracted the corresponding $n$ values would be 0.34, 0.49 and 0.30 with no logic in variation and no indication to the role of matrix dissolution in the release. The release results show that the spray-dried $SiO_2$ microparticles are dense enough to stop the extensive out-diffusion of propranolol after the initial faster release and the $SiO_2$ dissolution is needed.

The propranolol release from the low water-to-TEOS ratio microparticles, Bs16–18, was similar *in sink* conditions and in the $SiO_2$-saturated buffer (not shown). Propranolol was totally released from all specimens after 20 h of dissolution in both buffers. The matrix dissolution is also very fast as seen in Fig. 2. The release of propranolol is slightly slower than the release of BSA from the corresponding microparticles, indicating better encapsulation for propranolol than for BSA.

The amount of released propranolol from the monoliths with a low water-to-TEOS ratio $R_1 = 3$ (Fig. 7) into the $SiO_2$-saturated buffer are 9, 15 and 23 wt.% for Bm13, Bm14 and Bm15, respectively. *In sink* conditions the release is faster and continues as a function of time. The difference to the monolith formulations made at high water-to-TEOS ratios, $R = 30$ (Am06–08, Figs. 4 and 5) is clear. The release rates of propranolol from $R = 3$ monoliths are substantially lower and the role of matrix dissolution is clearly observed. The difference between the *in sink* conditions and $SiO_2$-saturated buffer results suggests that propranolol is partly encapsulated in closed pores of Bm13–15

Table 3
Calculated $M_2$, $t_2$, $n_B$, and $\ln k$ according to the new modified power law $(M_t - M_2)/M_\infty = k(t - t_2)^{n_B}$ for propranolol release in Tris (*in sink* conditions) and in $SiO_2$ saturated Tris-buffer

| Sample name | Propranolol release in Tris | | | | | Propranolol release in $SiO_2$ saturated Tris | | | | |
|---|---|---|---|---|---|---|---|---|---|---|
| | $M_2$ (%) | $t_2$ (h) | $n_B$ | $\ln k$ | $R$ | $M_2$ (%) | $t_2$ (h) | $n_B$ | $\ln k$ | $R$ |
| Am06 | 35.4 | 12 | 0.50 | 0.99 | 0.99 | 32.7 | 12 | 0.57 | 0.73 | 0.98 |
| Am07 | 40.8 | 12 | 0.51 | 0.95 | 0.98 | 40.4 | 12 | 0.47 | 1.11 | 0.98 |
| Am08 | 45.6 | 12 | 0.46 | 1.16 | 0.98 | 41.9 | 12 | 0.50 | 0.95 | 0.98 |
| As09 | 12.9 | 220 | 1.00 | −4.11 | 0.99 | – | – | – | – | – |
| As10 | 27.5 | 220 | 0.86 | −2.78 | 0.98 | – | – | – | – | – |
| As11 | 51.3 | 220 | 0.74 | −2.28 | 0.97 | – | – | – | – | – |
| Bm13 | 20.1 | 338 | 0.60 | −1.94 | 0.97 | – | – | – | – | – |
| Bm14 | 27.9 | 338 | 0.62 | −1.76 | 0.97 | – | – | – | – | – |
| Bm15 | 33.2 | 338 | 0.66 | −2.08 | 0.98 | – | – | – | – | – |

and $SiO_2$ has to dissolve before drug release occurs. However, the overall matrix dissolution is slower than drug release and the release rate decreases quite a lot towards the end. In other words, the release profiles suggest that diffusion has a major role in the release. The power law does not give reasonable fitting without the burst subtraction. The release deviates substantially from the main phase until 338 h. After 338 h the $n_B$ values show anomalous diffusion ($n_B = 0.6 \pm 0.06$, Table 3), i.e., mainly diffusion-controlled release.

## 4. Discussion

Dissolution experiments done in saturated and unsaturated conditions provides results that show the general release mechanism of the system. Clearly diffusion-controlled system has similar release behaviour in both buffers and in matrix erosion controlled system no release is observed in saturated buffer. The use of two buffers provided also information about internal structure and encapsulation ability of the matrix. In the case of propranolol release from monoliths (Am06–08) with high initial $R$ the drug release in both buffers was very similar indicating diffusion controlled system. Whereas in the case of low $R$ monoliths (Bm13–15) matrix degradation had an effect on drug release, suggesting that propranolol was partly capsulated into the closed pores.

In addition, difference in release was observed between small propranolol and larger BSA. No BSA release was observed in the $SiO_2$-saturated buffer, but the conditions allowing free dissolution of $SiO_2$ matrix showed release of BSA in the case of monoliths and microparticles (Fig. 3). Microparticle formulations with $R_1 = 2$ could not encapsulate BSA (Bs05) or propranolol (Bs16–18) into matrix to achieve controlled release. The difference in the matrix degradation in BSA and propranolol containing microparticles prepared at high water-to-TEOS ratio indicates that the initial matrix degradation is slower for BSA containing microparticles. BSA is larger than propranolol and a greater heterogeneity in $SiO_2$ structure could be a reasonable conclusion. However, the larger size of BSA may result in slower diffusion to the exterior of the droplet during the spray drying. In addition, the interaction between $SiO_2$ and propranolol and between $SiO_2$ and BSA, respectively may differ a lot, both during the $SiO_2$ preparation at lower $pH_1$ 2–2.8 (propranolol) and $pH_2$ 5–6 (BSA) and during the release of both molecules at pH 7.4. Propranolol is quite hydrophilic at the used synthesis pH 2–2.8, positively-charged ($pK_a = 9.4$) and it contains two active sites for hydrogen bonding, both donors, NH and OH, and they are located near each other. The isoelectric point of $SiO_2$ is near the synthesis pH, but propranolol has still possibilities to interact with Si–OH by hydrogen bonding. The release results of propranolol from the monolith with high water-to-TEOS ratio support suggestion on the weak interaction at pH 7.4 (Figs. 5 and 6), although propranolol is still fully dissociated and positively charged and $SiO_2$ is negatively charged. Hydrophilic $SiO_2$ is also known to adsorb BSA on its surface near the isoelectric point of BSA (pH 4.7) and still a substantial amount at neutral pH (although less than at pH 4.7), despite the negative net charge of BSA (Norde and Favier, 1992). At high water-to-TEOS ratios the water amount is large enough for homogeneous distribution of BSA in general and the interaction is suggested to be stronger than between propranolol and $SiO_2$, which results in more homogeneous distribution than in the case of propranolol.

Due to relatively often observed burst and lag time, we suggest a modified power law (Eq. (2)) which takes into account both of these possible initial release phases that differ from the main release phase. The $n_B$ values calculated according to the suggested modifications in the power law are sensitive to the chosen point that separates the initial release phase from the actual release phase. However by using combinatory data, i.e., by evaluating the physical meaning of $n$ values obtained from the power law without any burst or lag time subtractions, by comparing the data obtained from the use of dissolution media with free matrix dissolution and prevented matrix dissolution, and by analysing different time ranges in the release curves, it is possible to choose a justified point representing the start of the main release phase.

One could argue that the observation on any burst or lag time indicates that the power law cannot be used because one of the main prerequisites is that the distribution of the drugs should be homogeneous. However, the burst and lag time might also depend on the heterogeneous structure of the matrix containing a homogeneously distributed drug. This is an obvious option for sol–gel derived $SiO_2$ that consists of aggregated nanoparticles, where both larger amounts of drugs and larger drugs may disturb the homogeneity of the matrix nanostructure. Also heterogeneous drug distribution is possible. The $SiO_2$ structure shrinks during the aging and drying and water and other liquids diffuse out spontaneously, by capillary forces or by vapour Knudsen diffusion (Brinker and Scherer, 1990) and thus, drug migration is also possible.

In conclusion, it was shown that the use of dissolution medium allowing free dissolution of the matrix combined with the use of medium preventing the dissolution provides general information about the release mechanism. A modified power law is suggested. It takes into account an initial release phase, either burst or lag time that differ from the main release phase. The release results obtained from the modified power law supported the results obtained from the use of the different dissolution media. It was shown that diffusion is the main mechanism controlling the release of small-sized propranolol from the $SiO_2$ monolith matrices. Despite of the main role of the diffusion, the $SiO_2$ matrix dissolution had a clear effect on the release of monoliths made at low water-to-TEOS ratios. The release rate from the monoliths could also be substantially adjusted by formulation. The model protein, BSA, was successfully encapsulated both into monoliths and microparticles prepared with high water-to-TEOS ratio and the release was shown to occur predominantly by matrix erosion.

## Acknowledgements

Runar Bäckström Foundation, National Technology Agency of Finland (TEKES), and “Stiftelsens för Åbo Akademi Forskningsinstitut” are acknowledged for financing this study and

authors wish to thank BSc Merja Leino for the technical assistance.

## References


Ahola, M., Kortesuo, P., Kangasniemi, I., Kiesvaara, J., Yli-Urpo, A., 2000. Silica xerogel carrier material for controlled release of toremifene citrate. Int. J. Pharm. 195, 219–227.

Ahola, M.S., Säilynoja, E.S., Raitavuo, M.H., Vaahtio, M.M., Salonen, J.I., Yli-Urpo, A.U.O., 2001. *In vitro* release of heparin from silica xerogels. Biomaterials 22, 2163–2170.

Al-Saraj, M., Abdel-Latif, M.S., El-Nahal, I., Baraka, R., 1999. Bioaccumulation of some hazardous metals by sol–gel entrapped microorganisms. J. Non-cryst. Solids 248, 137–140.

Andrade, J.S., Street, D.A., Shibusa, Y., Havlin, S., Stanlay, H.E., 1997. Diffusion and reaction in percolating pore networks. Phys. Rev. 55, 772–777.

Arnir, D., Braun, S., Lev, O., Ottolenghi, M., 1994. Enzymes and other proteins entrapped in sol–gel materials. Chem. Mater. 6, 1605–1614.

Bhatia, R.B., Brinker, C.J., Gupta, A.K., Singh, A.K., 2000. Aqueous sol–gel process for protein encapsulation. Chem. Mater. 12, 2434–2441.

Böttcher, H., Slowik, P., Süss, W., 1998. Sol–gel carrier systems for controlled drug delivery. J. Sol–Gel Sci. Technol. 13, 277–281.

Brinker, C.J., Scherer, G.W., 1990. Sol–Gel Science: The Physics and Chemistry of Sol–Gel Processing. Academic Press, San Diego.

Brown, J.R., Shockley, P., 1982. Serum albumin: structure and characterization of its ligands binding sites. In: Jost, P.C., Griffith, O.H. (Eds.), Lipid-protein interactions, vol. 1. Wiley, New York, pp. 25–68.

Conroy, J.F.T., Power, M.E., Martin, J., Earp, B., Hosticka, B., Daitch, C.E., Norris, P.M., 2000. Cells in sol–gels. I. A cytocompatible route for the production of macroporous silica gels. J. Sol–gel Sci. Technol. 18, 269–283.

Flora, K.K., Brennan, J.D., 2001. Effect of matrix aging on the behavior of human serum albumin entrapped in a tetraethyl orthosilicate-derived glass. Chem. Mater. 13, 4170–4179.

Friedli, G.L., 1996. Interaction of deamidated soluble wheat protein with other food proteins and metals. Doctoral Thesis. University of Surrey.

Göpferich, A., Langer, R., 1995. Modeling monomer release from bioerodible polymers. J. Control. Rel. 33, 55–69.

Göpfrich, A., 1997. Erosion of composite polymer matrices. Biomaterials 18, 397–403.

Harland, R.S., Dubernet, C., Benoît, J.B., Peppas, N.A., 1988. A model of dissolution-controlled, diffusional drug release from non-swellable polymeric microspheres. J. Control. Rel. 7, 207–215.

Higuchi, T., 1961. Rate of release of medicaments from ointment bases containing drugs in suspension. J. Pharm. Sci. 50, 874–875.

Huang, X., Brazel, C.S., 2001. On the importance and mechanism of burst release in matrix-controlled drug delivery systems. J. Control. Rel. 73, 121–136.

Kadnikova, E.N., Kostic, N.M., 2001. Sol–gel glass is not necessarily an inert matrix for enzyme encapsulation. Catalysis of sulfoxidation by silica. J. Non-cryst. Solids 283, 63–68.

Keeling-Tucker, T., Rakic, M., Spong, C., Brennan, J.D., 2000. Controlling the materials properties and biological activity of lipase within sol–gel derived bioglass via organosilane and polymer doping. Chem. Mater. 12, 3695–3704.

Kortesuo, P., Ahola, M., Karlson, S., Kangasniemi, I., Yli-Urpo, A., Kiesvaara, J., 2000a. Silica xerogel as an implantable carrier for controlled drug delivery—evaluation of drug distribution and tissue effects after implantation. Biomaterials 21, 193–198.

Kortesuo, P., Ahola, M., Kangas, M., Kangasniemi, I., Yli-Urpo, A., Kiesvaara, J., 2000b. *In vitro* evaluation of sol–gel processed spray dried silica gel microspheres as carrier in controlled drug delivery. Int. J. Pharm. 200, 223–229.

Kortesuo, P., Ahola, M., Kangas, M., Leino, T., Laakso, S., Vuorilehto, L., Yli-Urpo, A., Kiesvaara, J., Marvola, M., 2001a. Alkyl-substituted silica gel as a carrier in the controlled release of dexmedetomidine. J. Control. Rel. 76, 227–238.

Kortesuo, P., Ahola, M., Kangas, M., Yli-Urpo, A., Kiesvaara, J., Marvola, M., 2001b. *In vitro* release of dexmedetomidine from silica xerogel monoliths: effect of sol–gel synthesis parameters. Int. J. Pharm. 221, 107–114.

Koskinen, M., Säilynoja, E., Ahola, M., Jalonen, H., Salonen, J., Kähäri, V.M., 2002. Biodegradable carrier and method for preparation thereof. WO 02/080977 A1, Patent Application, Oct 17.

Koskinen, M., Toriseva, M., Ahonen, M., Kähäri, V.M., Salonen, J.I., 2003. Release of recombinant adenoviruses from silica sol–gel *in vitro* and *in vivo*. In: Proceedings of the 30th Annual Meeting on Controlled Release Society, Glasgow, UK.

Kumar, A.V.A., Yashonath, S., 2000. Effect of a distribution of pore dimension on levitation effect. J. Phys. Chem. B 104, 9126–9130.

Lai, W., Ducheyne, P., Garino, J., 1998. Removal pathway of silicon released from bioactive glass granules *in vivo*. In: Geros, R.Z., LeGeros, J.P. (Eds.), Proceedings of the 11th International Symposium on Ceramics in Medicine, Bioceramics, vol. 11, pp. 383–386.

Lee, J.W., Gardella, J.A., Hicks, W., Hard, R., Bright, F.V., 2003. Analysis of the initial burst of drug release coupled with polymer surface degradation. Pharm. Res. 20, 149–152.

Meseguer-Olmo, L., Ros-Nicolás, M.J., Clavel-Sainz, M., Vicente-Ortega, V., Alcaraz-Baños, M., Lax-Pérez, A., Arcos, D., Ragel, C.V., Vallet-Regí, M., 2002. Biocompatibility and *in vivo* gentamicin release from bioactive sol–gel glass implants. J. Biomed. Mater. Res. 61, 458–465.

Nicoll, S.B., Radin, S., Santos, E.M., Tuan, R.S., Ducheyne, P., 1997. *In vitro* release kinetics of biologically active transforming growth factor-beta1 from a novel porous glass carrier. Biomaterials 18, 853–859.

Norde, W., Favier, J.P., 1992. Structure of adsorbed and desorbed proteins. Colloid Surf. 64, 87–93.

Peppas, N.A., 1985. Analysis of Fickian and non-Fickian drug release from polymers. Pharm. Acta Helv. 60, 110–111.

Pope, E.J.A., Braun, K., Peterson, C.M., 1997. Bioartificial organs. I. Silica gel encapsulation pancreatic islets for the treatment of diabetes mellitus. J. Sol–Gel Sci. Technol. 8, 635–639.

Radin, S., Ducheyne, P., Kamplain, T., Tan, B.H., 2001. Silica sol–gel for the controlled release of antibiotics. I. Synthesis, characterization, and *in vitro* release. J. Biomed. Mater. Res. 57, 313–320.

Santos, E.M., Radin, S., Ducheyne, P., 1999. Sol–gel derived carrier for the controlled release of proteins. Biomaterials 20, 1695–1700.

Sglavo, V.M., Carturan, G., dal Monte, R., Muraca, M., 1999. $SiO_2$ entrapment of animal cells. J. Mater. Sci. 34, 3587–3590.

Siepmann, J., Göpferich, A., 2001. Mathematical modeling of bioerodible, polymeric drug delivery systems. Adv. Drug Del. Rev. 48, 229–249.

Siepmann, J., Peppas, N.A., 2001. Modeling of drug release from delivery systems based on hydroxypropyl methylcellulose (HPMC). Adv. Drug Del. Rev. 48, 139–157.

Tamada, J.A., Langer, R., 1993. Erosion kinetics of hydrolytically degradable polymers. Proc. Natl. Acad. Sci. U.S.A. 90, 552–556.

Viitala, R., Jokinen, M., Tuusa, S., Rosenholm, J.B., Jalonen, H., 2005a. Adjustably bioresorbable sol–gel derived $SiO_2$ matrices for release of large biologically active molecules. J. Sol–Gel Sci. Technol. 36, 147–156.

Viitala, R., Jokinen, M., Maunu, S.L., Jalonen, H., Rosenholm, J.B., 2005b. Chemical characterization of bioresorbable sol–gel derived $SiO_2$ matrices prepared at protein-compatible pH. J. Non-cryst. Solids 351, 3225–3234.